The Korean Journal of Ceramics, **6**[3] 258-261 (2000)

Crystal Structure and Dielectric Responses of Pulsed Laser Deposited (Ba, Sr)TiO_3 Thin Films with Perovskite $LaNiO_3$ Metallic Oxide Electrode

Su-Jae Lee, Kwang-Yong Kang, Sang-Don Jung, Jin-Woo Kim and Seok-Kil Han

Research Department, Electronics and Telecommunications Research Institute, Taejon, 305-350, Korea

(Received September 23, 1998)

Highly (h00)-oriented (Ba, Sr)TiO_3 (BST) thin films were grown by pulsed laser deposition on the perovskite $LaNiO_3$(LNO) metallic oxide layer as a bottom electrode. The LNO films were deposited on SiO_2/Si substrates by rf-magnetron sputtering method. The crystalline phases of the BST film were characterized by x-ray θ-2θ, ω-rocking curve and φ-scan diffraction measurements. The surface microsturcture observed by scanning electron microscopy was very dense and smooth. The low-frequency dielectric responses of the BST films grown at various substrate temperatures were measured as a function of frequency in the frequency range from 0.1 Hz to 10 MHz. The BST films have the dielectric constant of 265 at 1 kHz and showed multiple dielectric relaxation at the low frequency region. The origin of these low-frequency dielectric relaxation are attributed to the ionized space charge carriers such as the oxygen vacancies and defects in BST film, the interfacial polarization in the grain boundary region and the electrode polarization. We studied also on the capacitance-voltage characteristics of BST films.

Key words: (Ba, Sr)TiO_3 thin film, $LaNiO_3$, Dielectric relaxation, Space chargr carrier

I. Introduction

Barium strontium titanate[(Ba_x, Sr_{1-x})TiO_3, (BST)] is one of the most promising candidates for 1 Gbit dynamic random access memories (DRAMs) capacitor. For the application of this material as a dielectric capacitor, electrode materials are required to have certain properties such as high metallic conductivity, sufficient resistance against oxidation, good adhesion to BST, and interfacial smoothness to achieve large capacitance and low leakage current. Some perovskite oxides are highly conductive and stable at high temperature even in oxygen-containing atmosphere. Futhermore, some of them have lattice constants similar to those of BST and better lattice matching can be expected at the interface between BST and electrodes, which may eliminate interfacial defects and additional electronic states at the interface and reduce the leakage current or the dielectric degradation. Recently, the conducting perovskite oxides such as $YBa_2Cu_3O_{7-\delta}$, $La_{0.5}Sr_{0.5}CoO_3$, and $SrRuO_3$ were employed as electrodes in epitaxially grown single crystal capacitors and they manifested higher qualities such as higher dielectric constants for paraelectric capacitors or higher fatigue resistances for ferroelectric capacitors.[1-4] On the other hand, some attentions have been focused on the fabrication of perovskite oxide $LaNiO_3$(LNO) thin films.[5-7] Because the LNO has a structure similar to that of perovskite ferroelectric, the textured LNO films has been used as a bottom electrode for the growth of (100)-oriented ferroelectric films on Si substrates, such as Pb(Zr, Ti)O_3(PZT).[8] $LaNiO_3$ is a perovskite-type metallic oxide with a lattice parameter of 3.84 Å. The resistivity of $LaNiO_3$ is isotropic and low(2.25×10^{-4} Ω·cm), and the temperature dependence indicates a good metallic behavior.[9]

In this letter, we report on the crystalline structures and dielectric responses of BST thin films deposited on electrodes of LNO film by pulsed laser deposition (PLD).

II. Experimental

The LNO thin films was deposited on the (100) surface of silicon substrates using radio frequency magnetron sputtering technique.[8] The $LaNiO_3$ target with 2-inch diameter were made by using a conventional mixed-oxide method, which included calcination at 900°C for 4 hours and sintering at 1000°C for 2 hours. Sputtering was carried out at a power density of 2.5 W/cm^2 and a working pressure of 10 mTorr with a gas ratio of Ar/O_2(15/3). The substrate temperature during deposition was kept at 300°C. We confirmed that the LNO films have a highly (100)-oriented perovskite phase by x-ray diffraction analysis.

($Ba_{0.5}Sr_{0.5}$)TiO_3 thin films were grown by the pulsed laser deposition on LNO(100)/SiO_2/Si substrates. The energy fluence was 2 J/cm^2 and the target to substrate distance was kept at 45 mm. The films were deposited at the temperatures of 500-700°C under 200 mTorr oxygen pressure. A growth rate was approximately 1 Å/pulse.

The crystallographic structures of BST films were analyzed by x-ray diffraction(XRD) using a characteristic x-ray

of Cu-Kα. In addition to θ-2θ diffraction, rocking curve measurements and φ-scan diffraction were carried out. The surface morphology and the thickness of the BST film were examined by scanning electron microscopy.

The dielectric properties of the BST films were studied for the capacitors with metal-insulator-metal (MIM) device configuration. Au top electrodes of 2000 Å in thickness and 1 mm^2 in area were deposited through a shadow mask at room temperature. LNO films were used for the bottom electrodes. The bias voltage dependence of the capacitance and the dielectric loss were measured using a computer-controller impedance analyzer(HP4194A) at 10 kHz and 0.5 V_{rms} oscillation voltage. The frequency dependence of complex impedance was measured by an impedance gain/phase analyzer (Solartron SI-1260) in the frequency range from 0.1 Hz to 10 MHz. The complex dielectric constants of BST films were calculated from the measured complex impedance.

III. Results and Discussions

BST film orientation with respect to the LNO/SiO_2/Si substrates and the temperature dependence of the unit-cell parameters were determined by XRD. Figure 1 shows the θ-2θ diffraction patterns of the BST films deposited at different substrate temperatures. All the films showed a highly (100)-oriented pervskite phases. However, the film deposited at 500°C had a much weaker intensity of diffraction peaks. At the growth temperature of 500°C, BST films started to form a perovskite phase. BST films deposited at temperatures of 600°C, 650°C, and 700°C exhibited good crystallinity as shown in Fig. 1. The presence of only (100) and (200) diffraction lines of BST film on LNO film suggests that the BST film is either highly (100)-oriented or grown epitaxially on the LNO(100)/SiO_2/Si substrates. The d(100) spacing obtained from the (100) peak of BST films was 3.951 Å, which is close to that of bulk BST(a=3.947 Å). This value was constant at the deposition temperature.

To confirm the epitaxial growth and crystallinity of BST films, ω-rocking curve and φ-scan diffraction measurements were carried out. Figure 2(a) is the x-ray rocking curve obtained on the (200) diffraction line of the BST film grown at 650°C. The solid line is fitted by Gaussian function. The full width at half maximum (FWHM) is estimated to be around 1.69°. Profiles of φ-scan diffraction were measured for (101) plane of the BST film. In Fig. 2(b), four equally spaced peaks separated by 90° are seen. Thus, this clearly suggests that the BST film with perovskite structure is epitaxially grown on the LNO film substrate.

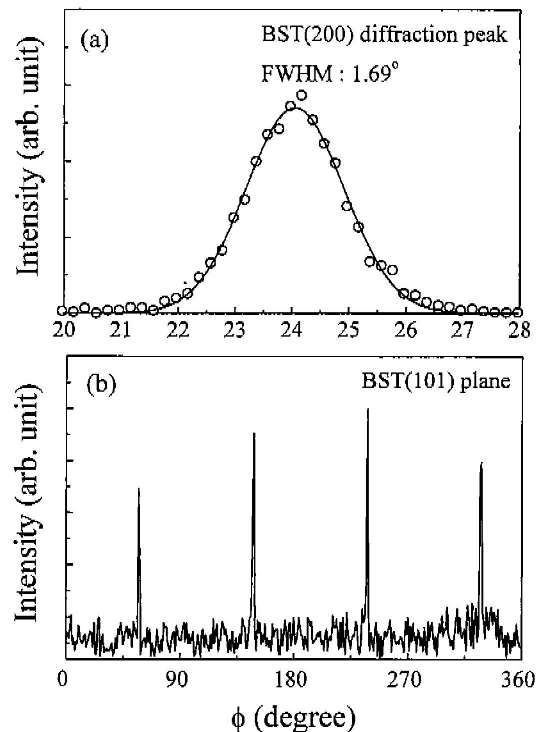

Fig. 2. (a) Rocking curve for BST(200) diffraction line and (b) φ-scan diffraction for the BST(101) plane of the BST film.

We studied the microscopic surface morphology of the BST films using scanning electron microscopy (SEM). Figure 3 shows the typical SEM image of BST film deposited at

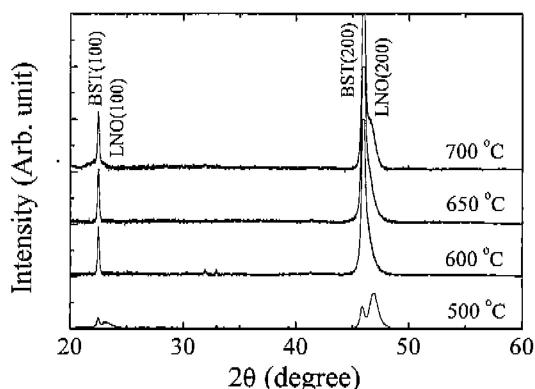

Fig. 1. X-ray θ-2θ diffraction patterns for the BST films on LNO/SiO_2/Si substrates.

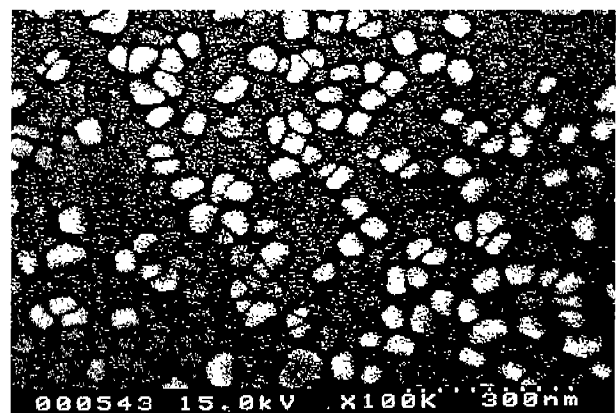

Fig. 3. Surface morphology for the BSTO film deposited at 650°C.

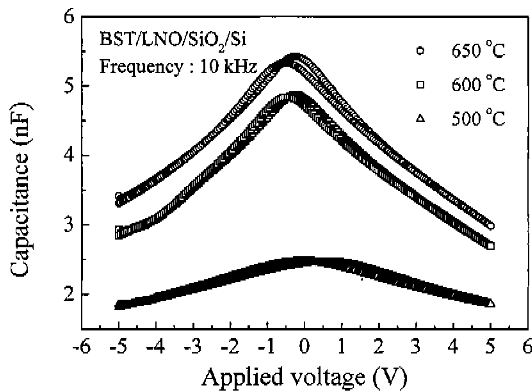

Fig. 4. Bias voltage dependence of capacitance(C-V curves) measured for the BSTO films with substrate temperature.

temperature of 650°C. The BST surface was very smooth and dense without showing any pin-holes as shown in Fig. 3. The grains were round in shape and uniform in size (~0.04 μm).

Figure 4 shows the bias voltage dependence of the capacitance for BST films deposited at several temperatures. The thickness of the film was 3000 Å. The capacitance-voltage (C-V) curves were measured at the frequency of 10 kHz with a small amplitude of 0.5 V, while the dc bias voltage was swept from negative bias(−5V) to positive bias(+5V) at a sweep rate of 0.1 V/sec and back again. The capacitance of the films increased with increasing the deposition temperature, and exhibited a strong nonlinearity on an applied voltage. The maximum values of the capacitance were taken at about zero voltage. The C-V curves showed a small hysteresis, which indicates that they contain a few movable ions or charge accumulation at the interface between the film and the electrodes.

The dielectric properties of BST films were investigated at a frequency range of 0.1 Hz~10 MHz. Figure 5(a) and (b) show the frequency dependence of the real part ε' and imaginary part ε'' of the complex dielectric constant for BST(100) films deposited on the LNO film at the growth temperature of 500°C, 600°C and 650°C, respectively. The measurement was performed at room temperature. The value of real ε' increased with increasing the growth temperature, which was 265 at 1 kHz. All the films exhibited a remarkable dielectric dispersion in the frequency range from 0.1 Hz to 10 MHz and showed multiple dielectric relaxations with peaks in the imaginary dielectric constant of the films. A peak in the imaginary dielectric constant of BST films grown above 600°C is observed at around 22 Hz and 150 kHz, and that for BST films grown at 500°C is shifted to higher frequencies. Dielectric relaxation represents the charge in polarization of a material according to a time-variant applied field. It depends upon frequency as various mechanism responsible for polarization are effective at different frequencies. In dielectric materials, four different mechanism are possible: electronic polarization, atomic polarization, dipolar polarization, and space charge polarization or interfacial polarization.

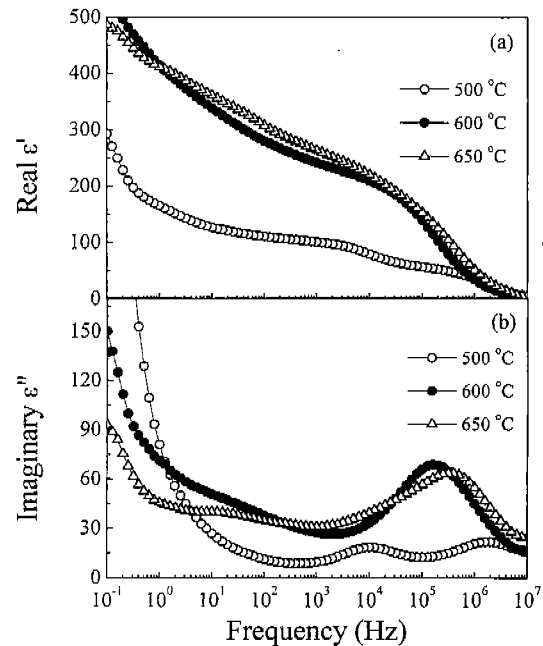

Fig. 5. Frequency dependence of the complex dielectric constant for the BSTO films deposited at 500°C, 600°C and 650°C. (a) real (ε'), and (b) imaginary (ε'') dielectric constant.

Electronic and atomic relaxations are related to very rapid oscillations of weak dipoles, and are only measurable at high frequencies (>10^{10} Hz). If the materials possess preferably orientated dipoles, the subsequent dipolar relaxations appear at audio frequency range from 10 Hz to 10 MHz. Practically, the dielectric properties are strongly influenced by the presence of moisture, by the complexity of the grain boundaries, by the various grain size and orientation, and by an ionic space-charge carriers. Thus, this dielectric relaxations occurring in the low frequency region can be related to ionic space-charge carriers such as the oxygen vacancies and a defect generated during film growth, the interface polarization located on grain boundary and the interface between the film and electrode, and electrode polarization. The role of oxygen vacancies($V_o^{\cdot\cdot}$)and their related defects are often the proposed culprits in various reliability limiting processes of oxide perovskite materials. The $V_o^{\cdot\cdot}$ is doubly charged with respect to the neutral lattice and is considered to be the most mobile intrinsic ionic defect in these materials. It is considered that oxygen vacancies act as donors in BST film, as follows: $O_o=V_o^{\cdot\cdot}+2e^-+1/2O_2$, where O_o is oxygen ions at oxygen sites, $V_o^{\cdot\cdot}$ ionized oxygen vacancies, and e electron. Based on comprehensive studies of crystalline strontium titanate by Waser and co-worker,[10,11] it has often been suggested that the oxygen vacancy plays an important role in the resistance degradation and dielectric degradation of thin polycrystalline BST films. Also, Warren reported that the $V_o^{\cdot\cdot}$-related defect dipoles in perovskite oxides are aligned along the applied external field direction.[12] The paraelectric $BaTiO_3$ single crystal exhibits the low-frequency relaxation attributed to anisotropic conduc-

tivity or Debye-like relaxation from dipoles arising from defects in the crystal lattice[13] and surface.[14] The ultralow frequency (~1 Hz) relaxation observed in polycrystalline $SrTiO_3$ and $BaTiO_3$ at T>Tc is due to Maxwell-Wagner interfacial relaxation arising from the capacitive grain boundaries and the resistive grains present in the microstructure.[15] As is shown in Fig. 5, these dielectric relaxation phenomena in the low frequency are attributed to the dielectric rotation of $V_o^{\cdot\cdot}$-related defect dipoles in grains, the interfacial polarization at the grain boundaries and the electrode polarization with long-range movements of space charge carriers. Due to the increase of electrical conductivity at low frequency below 10 Hz, both ε' and ε" tend to increase as the frequency decreases below 10 Hz.

IV. Conclusions

Highly (100)-oriented BST films were successfully grown on conductive metallic oxide $LaNiO_3$(100) films at various temperatures by pulsed laser deposition. LNO film provides not only a bottom electrode for BST but also an excellent seed layer for epitaxial growth of BST on it. The surface microstructure of BST film was dense and smooth. BST thin film deposited at 650°C has a dielectric constant around 265 at 1 kHz. The dielectric properties of BST films showed a remarkable dielectric dispersion and multiple dielectric relaxation at the frequency range from 0.1 Hz to 10 MHz. The present dielectric relaxation was interpreted on the basis of dielectric rotation of $V_o^{\cdot\cdot}$-related defect dipoles in grains, the interfacial polarization at the grain boundary region and the electrode polarization with long-range movements of space charge carriers.

References

1. Q. X. Jia, X. D. Dw, S. R. Foltyn and P. Tiwari, *Appl. Phys. Lett.*, **66**, 2197 (1995).
2. M. Izuha, K. Abe, M.Koike, S. Takeno and N Fukushima, *Appl. Phys. Lett.*, **70**, 1405 (1997).
3. N. J. Wu, H. Lin, K. Xie, X. Y. Li and A. Ignatiev, Physica C, **232**, 151 (1994).
4. H. N. Al-Shareef, B. A. Tuttle, W. L. Warren, D. Dimos, M. V. Raymond and M. A. Rodriguez, *Appl. Phys. Lett.*, **68**, 272 (1996).
5. K. M. Satyalakshmi, R. M. Mallya, X. D. Wu, B. Brainard and D. C. Gautier, *Appl. Phys. Lett.*, **62**, 1233 (1993).
6. H. Ichinose, Y. Shiwa and M. Nagano, *Jpn. J. Appl. Phys.*, **33**, 5907(1994).
7. H. Y. Lee, T. B. Wu and J. F. Lee, *J. Appl. Phys.*, **80**, 2175 (1996).
8. B. G. Chae, S. J. Lee, S. H. Kim, Y. S. Yang and M. S. Jang, *J. Kor. Phys. Soc.*, **32**, S1438 (1998).
9. K. P. Rajeev, G. V. Shivashankar and A. K. Taychaudhun, *Solid State Communications* **79**, 591 (1991).
10. R. Waser, T. Baiatu and K. H. Hardtl, *J. Am. Ceram. Soc.*, **73**, 1645 (1990).
11. T. Baiatu. R. Waser and K. H. Hardtl, *J. Am. Ceram. Soc.*, **73**, 1663 (1990).
12. W. L. Warren, K. Vanheusden, D. Dimos and G. E. Pike and B. A. Tuttle, *J. Am. Ceram. Soc.*, **79**, 536 (1996)
13. T. Fernandez-Diaz, C. Prieto, J. L. Martinez, J. A. Gonalo and M. Aguilar, *Ferroelectrics*, **21**. 381 (1978).
14. R. Dudler, J. Albers and H. E. Muser, *Ferroelectrics*, **21**, 381 (1978).
15. H. Neumann and G. Arlt, *Ferroelectrics*, **69**, 179 (1986).